

Observation of nonadditive mixed state phases with polarized neutrons

Jürgen Klepp¹, Stephan Sponar¹, Stefan Filipp¹, Matthias Lettner¹, Gerald Badurek¹ and Yuji Hasegawa^{1,2}

¹Vienna University of Technology, Atominstitut, Stadionallee 2, 1020 Vienna, Austria and
²PRESTO, Japan Science and Technology Agency, 4-1-8 Honcho Kawaguchi, Saitama, Japan

(Dated: October 31, 2018)

In a neutron polarimetry experiment the mixed state relative phases between spin eigenstates are determined from the maxima and minima of measured intensity oscillations. We consider evolutions leading to purely geometric, purely dynamical and combined phases. It is experimentally demonstrated that the sum of the individually determined geometric and dynamical phases is not equal to the associated total phase which is obtained from a single measurement, unless the system is in a pure state.

PACS numbers: 03.65.Vf, 03.75.Be, 42.50.-p

Evolving quantum systems acquire two kinds of phase factors: (i) the dynamical phase which depends on the dynamical properties of the system - like energy or time - during a particular evolution, and (ii) the geometric phase which only depends on the path the system takes in state space on its way from the initial to the final state. Since its discovery by Pancharatnam [1] and Berry [2] the concept was widely expanded and has undergone several generalizations. Nonadiabatic [3] and noncyclic [4] evolutions as well as the off-diagonal case, where initial and final state are mutually orthogonal [5], have been considered. Ever since, a great variety of experimental demonstrations has been accomplished [6, 7], also in neutron optics [8, 9, 10, 11]. Due to its potential robustness against noise [12] the geometric phase is an excellent candidate to be utilized for logic gate operations in quantum information science [13]. Thus, a rigorous investigation of all its properties is of great importance.

In addition to an approach by Uhlmann [14] a new concept of phase for mixed input states based on interferometry was developed by Sjöqvist *et al.* [15]. Here, each eigenvector of the initial density matrix independently acquires a geometric phase. The total mixed state phase is a weighted average of the individual phase factors. This concept is of great significance for such experimental situations or technical applications where pure state theories may imply strong idealizations. Theoretical predictions have been tested by Du *et al.* [16] and Ericsson *et al.* [17] using NMR and single-photon interferometry, respectively. In this letter, we report on measurements of nonadiabatic and noncyclic geometric, dynamical and combined phases. These depend on noise strength in state preparation, defining the degree of polarization, the purity, of the neutron input state. In particular, our experiment demonstrates that the geometric and dynamical mixed state phases Φ_g and Φ_d , resulting from separate measurements, are not additive [18], because the phase resulting from a single, cumulative, measurement differs from $\Phi_g + \Phi_d$. This nonadditivity might be of practical importance for applications, e.g. the design of phase gates for quantum computation.

A neutron beam propagating in y -direction interact-

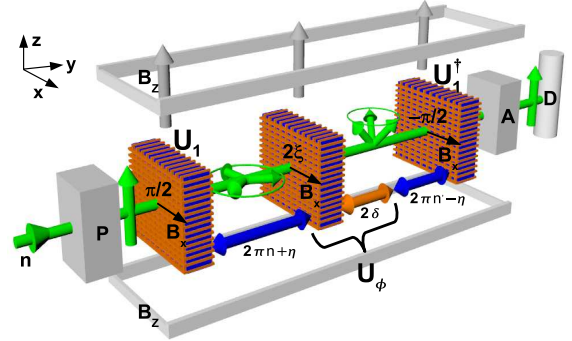


FIG. 1: Sketch of neutron polarimetry setup for phase measurement with overall guide field B_z , polarizer P, three DC-coils to implement unitary operations U_1 , U_1^\dagger , U_ϕ , analyzer A and detector D. Greek letters denote spin rotation angles. Shifting the second coil induces an additional dynamical phase η resulting in intensity oscillations. The desired phase ϕ is determined from their minima and maxima.

ing with static magnetic fields $\vec{B}(y)$ is described by the Hamiltonian $H = -\hbar^2/2m\vec{\nabla}^2 - \mu\vec{\sigma}\vec{B}(y)$; m and μ are the mass and the magnetic moment of the neutron, respectively. Zeeman splitting within $\vec{B}(y)$ leads to solutions of the Schrödinger equation $\cos(\theta/2)|k_+\rangle|+\rangle + e^{i\alpha}\sin(\theta/2)|k_-\rangle|-\rangle$, where $|k_\pm\rangle$ are the momentum and $|\pm\rangle$ the spin eigenstates within the field $\vec{B}(y)$. θ and α denote the polar and azimuthal angles determining the direction of the spin with respect to $\vec{B}(y)$. $k_\pm \simeq k_0 \mp \Delta k$, where k_0 is the momentum of the free particle and $\Delta k = m\mu|\vec{B}(y)|/\hbar^2k$ is the field-induced momentum shift. Δk can be detected from spinor precession. Omitting the coupling of momentum and spin, we focus on the evolution of superposed spin eigenstates resulting in Larmor precession of the polarization vector $\vec{r} = \langle\varphi|\vec{\sigma}|\varphi\rangle$, where $\vec{\sigma} = (\sigma_x, \sigma_y, \sigma_z)$ is the Pauli vector operator. The unitary, unimodular operator

$$U(\xi', \delta', \zeta') = e^{i\delta'} \cos \xi' |+\rangle\langle +| - e^{-i\zeta'} \sin \xi' |+\rangle\langle -| \\ + e^{i\zeta'} \sin \xi' |-\rangle\langle +| + e^{-i\delta'} \cos \xi' |-\rangle\langle -|$$

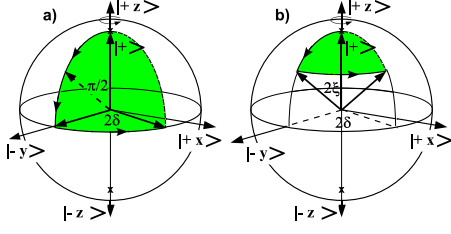


FIG. 2: Evolution of the $|+\rangle$ eigenstate induced by U_ϕ , associated to: a) Purely (noncyclic) geometric phase ($2\xi = \pi/2$). b) Combinations of dynamical and geometric phase on the Bloch sphere ($0 < 2\xi < \pi/2$).

describes the evolution of the system within static magnetic fields. The set of $SU(2)$ parameters (ξ', δ', ζ') is related to the so-called Cayley-Klein parameters a, b via $a = e^{i\delta'} \cos \xi'$ and $b = -e^{-i\zeta'} \sin \xi'$ (see e.g. [19]).

Consider the experimental setup shown in Fig. 1. A monochromatic neutron beam passes the polarizer P preparing it in the 'up' state $|+\rangle$ with respect to a magnetic guide field in z -direction (B_z). Next, the beam approaches a DC coil with its field B_x pointing to the x -direction. B_x is chosen such that it carries out the transformation $U_1 \equiv U(\pi/4, 0, -\pi/2)$, corresponding to a $+\pi/2$ rotation around the $+x$ -axis. After U_1 the resulting state of the system is a coherent superposition of the two orthogonal spin eigenstates: $|\psi_0\rangle = 1/\sqrt{2}(|+\rangle - i|-\rangle)$. A subsequent coil, represented by $U(\xi, 0, -\pi/2)$, is set to cause a spin rotation around the $+x$ -axis by an angle 2ξ . This second coil and the following propagation distance within B_z – corresponding to a rotation angle 2δ around

the $+z$ -axis – define an evolution $U_\phi \equiv U(\xi, \delta, \zeta)$. Undergoing the transformation U_ϕ the two spin eigenstates $|\pm\rangle$ acquire opposite total phase $\pm\phi = \pm \arg\langle \pm | U_\phi | \pm \rangle = \pm\delta$. A third coil (U_1^\dagger) reverses the action of the first one and would therefore transform a state $|\psi_0\rangle$ back to $|+\rangle$. The state of the system entering the third coil equals $|\psi_0\rangle$ only if $U_\phi = \mathbb{1}$. ϕ can be extracted by applying an extra dynamical phase shift $\pm\frac{1}{2}\eta$ to $|\pm\rangle$. It is implemented by adjusting both inter-coil distances from first to second and second to third coil to spin rotation angle equivalents of $2\pi n + \eta$ and $2\pi n' + 2\delta - \eta$ (n, n' are integer). By scanning the position of the second coil these rotation angles – referred to as $U_\eta \equiv U(0, \eta/2)$ and U_η^\dagger – are varied to yield intensity oscillations from which ϕ is calculated. Note that, because of $\xi' = 0$, the parameter ζ' is undetermined and, therefore, omitted in U_η . After projection on the state $|+\rangle$ by the analyzer A, the phase $\phi = \delta$ and its visibility $\nu = |\cos \xi|$ can be computed as functions of the maxima and minima of the intensity, I_{\max} and I_{\min} , measured by the detector D [20]. More general, a neutron beam with incident purity $r'_0 = |\vec{r}'_0|$ along the $+z$ -axis ($\vec{r}'_0 = (0, 0, r'_0)$) is described by the density operator $\rho_{\text{in}}(r'_0) = 1/2(\mathbb{1} + r'_0\sigma_z)$. Calculating $\rho_{\text{out}} = U_1^\dagger U_\eta^\dagger U_\phi U_\eta U_1 \rho_{\text{in}} U_1^\dagger U_\eta^\dagger U_\phi^\dagger U_\eta U_1$, we find the intensity

$$I^\rho \propto \frac{1 - r'_0}{2} + r'_0 (\cos^2 \xi \cos^2 \delta + \sin^2 \xi \cos^2(\zeta - \eta)) \quad (1)$$

after the analyzer A. Considering the maxima and minima $I_{\max}^\rho, I_{\min}^\rho$ of η -induced oscillations of I^ρ one obtains the mixed state phase [21]

$$\Phi(r'_0) = \arccos \sqrt{\frac{[I_{\min}^\rho/I_n^\rho - 1/2(1 - r'_0)]/r'_0}{r'_0[1/2(1 + r'_0) - I_{\max}^\rho/I_n^\rho] + [I_{\min}^\rho/I_n^\rho - 1/2(1 - r'_0)]/r'_0}} \quad (2)$$

with a normalization factor $I_n^\rho = 2I_0^\rho/(1 + r'_0)$. I_0^ρ is the intensity measured at $U_\phi = \mathbb{1}$.

The noncyclic geometric phase is given by $\phi_g = -\Omega/2$, where Ω is the solid angle enclosed by a geodesic path and its shortest geodesic closure on the Bloch sphere [4]: ϕ_g and the total phase ϕ are related to the path by the polar and azimuthal angles 2ξ and 2δ , so that the pure state geometric phase becomes

$$\phi_g = \phi - \phi_d = \delta[1 - \cos(2\xi)], \quad (3)$$

while its dynamical counterpart is

$$\phi_d = \delta \cos(2\xi). \quad (4)$$

By proper choice of 2ξ and 2δ , U_ϕ can be set to generate purely geometric, purely dynamical, or arbitrary combinations of both phases as shown in Fig. 2.

The theoretical prediction for the mixed state phase is [15, 21]

$$\Phi(r'_0) = \arctan(r'_0 \tan \delta) \quad (5)$$

To access Eq.(5) experimentally r'_0 needs to be varied. In addition to the DC current, which effects the transformation U_1 , random noise is applied to the first coil, thereby changing B_x in time. Neutrons, which are part of the ensemble $\rho_{\text{in}}(r'_0)$, arrive at different times at the coil and experience different magnetic field strengths. This is equivalent to applying different unitary operators $U(\pi/4 + \Delta\xi'(t), 0, -\pi/2) = \tilde{U}_1(\Delta\xi'(t))$. For the whole ensemble we have to take the time integral

$$\rho = \int \tilde{U}_1(\Delta\xi'(t)) |+\rangle \langle +| \tilde{U}_1^\dagger(\Delta\xi'(t)) dt.$$

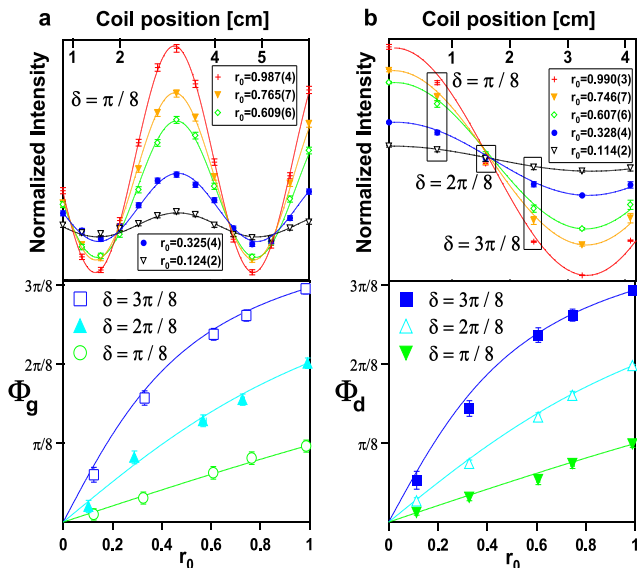


FIG. 3: Above: typical measured intensities for five values of purity r_0 versus coil positions. Below: resulting mixed state phases Φ_g and Φ_d versus purity r_0 . a) Purely geometric case: $2\xi = \pi/2$. Data indicated by circles is calculated from oscillations above. b) Purely dynamical case: $2\xi = 0$. Only one intensity value - marked by rectangles in the above plot - is needed for each Φ_d (see text).

Although each separate transformation is unitary, due to the randomness of the signal we end up with a nonunitary evolution that yields a mixed state [22]. Note that in this method the purity r'_0 of the input state is not affected before \tilde{U}_1 creates spin superpositions distributed around $|\psi_0\rangle$ within the y, z -plane. We are left with $\vec{r}_0 = (0, -r_0, 0)$ where $r_0 < 1$, as has been confirmed by a 3D spin analysis of the state $\tilde{U}_1 \rho_{\text{in}} \tilde{U}_1^\dagger$.

The experiment was carried out at the research reactor facility of the Vienna University of Technology. A neutron beam – incident from a pyrolytic graphite crystal – with a mean wavelength $\lambda \approx 1.98 \text{ \AA}$ and spectral width $\Delta\lambda/\lambda \approx 0.015$, was polarized up to $r'_0 \approx 99\%$ by reflection from a bent Co-Ti supermirror array. The analyzing supermirror was slightly de-adjusted to higher incident angles to suppress second order harmonics in the incident beam. The final maximum intensity was about 150 counts/s at a beam cross-section of roughly 1 cm^2 . A ^3He gas detector with high efficiency for neutrons of this energy range was used. Spin rotations around the $+x$ -axis were implemented by magnetic fields B_x from DC coils made of anodized aluminium wire (0.6 mm in diameter) wound on frames with rectangular profile ($7 \times 7 \times 2 \text{ cm}^3$). Coil windings in z -direction provided for compensation of the guide field B_z at coil positions (see Fig. 1) for B_x to be parallel to the x -direction. B_z was realized by two rectangular coils of 150 cm length in Helmholtz geometry. Maximum coil currents of 2 A and guide field strengths of 1 mT were sufficient to achieve required spin

rotations and prevent unwanted depolarization. The noise from a standard signal generator consisted of random DC offsets varying at a rate of 20 kHz. In order to find the coil current values for required spin rotation angles, each coil current was scanned separately. A measured intensity minimum after stepwise increase indicates that a π rotation has been achieved. Then, with both coils mounted on translation stages and set to a $\pi/2$ rotation around the x -axis, inter-coil distances were varied to search for intensity minima. The distance between two minima (6-7 cm in our case) corresponds to a 2π rotation around B_z within the x, y plane.

For purely geometric phases the parameter sets ($\xi = \pi/4, \delta, \zeta = \delta - \pi/2$) with $\delta = \phi_g = \pi/8, 2\pi/8, 3\pi/8$ were chosen. For each set the intensity oscillations I^p (see Fig. 3a, upper graph; data shown for $\delta = \phi_g = \pi/8$) were measured, scanning the position of the second coil for five values of r_0 . For the purely dynamical phase - since $2\xi = 0$ and Eq. (1) reduces to $I^p = (1 - r'_0)/2 + r'_0 \cos^2 \delta$ - only one intensity value is needed. With the second coil turned off, the distance between the first and the third coil was chosen such that $\delta = \phi_d = \pi/8, 2\pi/8, 3\pi/8$ for five values of r_0 (Fig. 3b, upper graph). By Eq. (2) the geometric and dynamical mixed state phases $\Phi_g(r_0)$ and $\Phi_d(r_0)$ (Fig. 3, lower graphs) were calculated from intensity values extracted from least square fits for I^p (solid lines in Fig. 3, upper graphs). Vertical error bars in the lower graphs contain two about equal contributions: fitting errors and an estimated uncertainty of 0.5 mm for the reproduction of coil positions. The small horizontal error bars stem from the statistical uncertainty of the purity measurements. The solid lines are theoretical curves according to Eq. (5), using the measured value for Φ without noise as phase reference. The experimental data reproduce well the r_0 -dependence predicted by Eq. (5).

We want to emphasize that our investigation focuses on a special property of the mixed state phase: its nonadditivity. Since the Sjöqvist phase is defined as a weighted average of phase factors rather than one of phases (see [18, 23] for a more elaborate discussion) it is true only for pure states that phases of separate measurements can be added up to a total phase. Suppose we carry out two measurements on a pure state system: the state is subjected to a unitary transformation U_g in the first and to U_d in the second measurement inducing the phases ϕ_g and ϕ_d , respectively. Applying Eqs. (3) and (4), we can also choose a combination of angles 2ξ and 2δ leading to a transformation U_{tot} so that we measure the total pure state phase $\phi_g + \phi_d$ (note that the three evolution paths induced by U_g, U_d and U_{tot} differ from each other). However, the result of the latter experiment for the system in a mixed state is $\Phi_{\text{tot}}(r_0) = \arctan[r_0 \tan(\phi_g + \phi_d)]$. The total phase is then *not* given by $\Phi_g(r_0) + \Phi_d(r_0)$, with $\Phi_g(r_0) = \arctan(r_0 \tan \phi_g)$ and $\Phi_d(r_0) = \arctan(r_0 \tan \phi_d)$. In our experiment we have chosen two examples of U_{tot} , i.e. two sets of values for B_x in the second coil ($2\xi^{(1)} = 60^\circ, 2\xi^{(2)} = 48^\circ$) and the distance within B_z ($2\delta^{(1)} =$

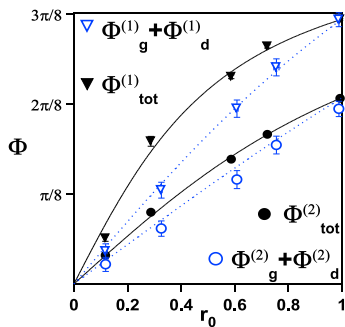


FIG. 4: Filled markers: Measured total mixed state phase Φ_{tot} versus purity r_0 for two examples of U_{tot} associated to the total pure state phases $\phi_g^{(1,2)} + \phi_d^{(1,2)}$ (see text). Open markers: $\Phi_g^{(1,2)} + \Phi_d^{(1,2)}$ as calculated from measured data in Fig. 3. The solid and dotted lines are theory curves assuming either nonadditivity or additivity, respectively. The data clearly demonstrate the nonadditivity of the Sjöqvist mixed state phase.

90° , $2\delta^{(2)} = 135^\circ$). According to Eqs. (3) and (4) the total pure state phases $\phi_g^{(1)} + \phi_d^{(1)}$ and $\phi_g^{(2)} + \phi_d^{(2)}$ with $\phi_g^{(1)} = \phi_g^{(2)} = \pi/8$ and $\phi_d^{(1,2)} = 2\pi/8, \pi/8$ are obtained from intensity oscillations. In Fig. 4 the resulting mixed state phases $\Phi_{\text{tot}}^{(1,2)}$ and the sum $\Phi_g^{(1,2)} + \Phi_d^{(1,2)}$ are plotted.

Note that this nonadditivity of mixed state phases is

not due to the nonlinearity of the geometric phase, that occurs – for instance – when the system evolves close to the orthogonal state of the reference state [24].

Recently there has been a report on NMR experiments [25] investigating Uhlmann’s mixed state geometric phase. It is a property of a composite system undergoing a certain non-local evolution of system and ancilla [26]. Diverse phase definitions, depending on this evolution, are possible. The phase investigated in the present paper is a special case in which the ancilla does not necessarily evolve. While the preconditions for inherent fault tolerance remain intact for the Sjöqvist phase, the question whether other phases offer advantages in terms of robustness remains an exciting issue of discussion.

To summarize, we have measured spin-1/2 mixed state phases with polarized neutrons. Their dependence on the purity of the input state was observed. Our results show that these phases are not additive. The sum of phases measured in separate experiments is not equal to the result of one single measurement, in contrast to what could be expected from straightforward extrapolation of pure state behavior. This interesting property of the Sjöqvist mixed state phase might be of high relevance for possible applications of geometric phases.

We thank E. Balcar for critical reading of the manuscript. This work was financed by the Japan Science and Technology Agency (JST) and the Austrian Science Fund (FWF, Project. Nr. P 17803-N02).

-
- [1] Pancharatnam, Proc. Indian Acad. Sci. A **44** (1956).
 - [2] M.V. Berry, Proc. R. Soc. Lond. A **392**, 45 (1984).
 - [3] Y. Aharonov and J.S. Anandan, Phys. Rev. Lett. **58**, 1593 (1987).
 - [4] J. Samuel and R. Bhandari, Phys. Rev. Lett. **60**, 2339 (1988).
 - [5] N. Manini and F. Pistolesi, Phys. Rev. Lett. **85**, 3076 (2000).
 - [6] A. Tomita and R.Y. Chiao, Phys. Rev. Lett. **57**, 937 (1986).
 - [7] D. Suter, K.T. Mueller and A. Pines, Phys. Rev. Lett. **60**, 1218 (1988).
 - [8] T. Bitter and D. Dubbers, Phys. Rev. Lett. **59**, 251 (1987).
 - [9] B.E. Allman *et al.*, Phys. Rev. A **56**, 4420 (1997).
 - [10] Y. Hasegawa *et al.*, Phys. Rev. Lett. **87**, 070401 (2001).
 - [11] S. Filipp, Y. Hasegawa, R. Loidl and H. Rauch, Phys. Rev. A **72**, 021602(R) (2005).
 - [12] P.J. Leek *et al.*, Science **318**, 1889 (2007).
 - [13] M.A. Nielsen and I.L. Chuang, *Quantum Computation and Quantum Information*, Cambridge University Press, Cambridge, England, 2000.
 - [14] A. Uhlmann, Lett. Math. Phys. **21**, 229 (1991).
 - [15] E. Sjöqvist *et al.*, Phys. Rev. Lett. **85**, 2845 (2000).
 - [16] J. Du *et al.*, Phys. Rev. Lett. **91**, 100403 (2003).
 - [17] M. Ericsson *et al.*, Phys. Rev. Lett. **94**, 050401 (2005).
 - [18] K. Singh *et al.*, Phys. Rev. A **67**, 032106 (2003).
 - [19] J.J. Sakurai, *Modern Quantum Mechanics* (Addison-Wesley, New York, 1994)
 - [20] A.G. Wagh and V.C. Rakhecha, Phys. Lett. A **197**, 112 (1995).
 - [21] P. Larsson and E. Sjöqvist, Phys. Lett. A **315**, 12 (2003); J. Klepp *et al.*, Phys. Lett. A **342**, 48 (2005); S. Sponar *et al.*, Acta Phys. Hung. A **26**, 165 (2006).
 - [22] R.A. Bertlmann, K. Durstberger and Y. Hasegawa, Phys. Rev. A **73**, 022111 (2006)
 - [23] Li-Bin Fu and Jing-Ling Chen, J. Phys. A: Math. Gen. **37**, 3699 (2004). E. Sjöqvist, J. Phys. A: Math. Gen. **37**, 7393 (2004). Li-Bin Fu and Jing-Ling Chen, J. Phys. A: Math. Gen. **37**, 7395 (2004).
 - [24] R. Bhandari, Phys. Rep. **281**, 1 (1997).
 - [25] J. Du *et al.*, arXiv:0710.5804v1 [quant-ph].
 - [26] M. Ericsson *et al.*, Phys. Rev. Lett. **91**, 090405 (2003).